Journal of ELECTRONIC MATERIALS, Vol. 46, No. 1, 2017
DOI: 10.1007/s11664-016-4866-x

Improved Piezoelectricity in $(K_{0.44}Na_{0.52}Li_{0.04})(Nb_{0.91}Ta_{0.05}Sb_{0.04})O_3$-$xBi_{0.25}Na_{0.25}NbO_3$ Lead-Free Piezoelectric Ceramics

YAN ZHAO,[1] ZHIJUN XU,[1,3,4] HUAIYONG LI,[1] JIGONG HAO,[1] JUAN DU,[1] RUIQING CHU,[1] DONGDONG WEI,[1] and GUORONG LI[2]

1.—College of Materials Science and Engineering, Liaocheng University, Liaocheng 252059, China. 2.—The State Key Lab of High Performance Ceramics and Superfine Microstructure, Shanghai Institute of Ceramics, Chinese Academy of Science, Shanghai 200050, China. 3.—e-mail: zhjxu@sohu.com. 4.—e-mail: zhjxu@lcu.edu.cn

$(1 - x)[(K_{0.44}Na_{0.52}Li_{0.04})(Nb_{0.91}Ta_{0.05}Sb_{0.04})O_3]$-$xBi_{0.25}Na_{0.25}NbO_3$ (KNLNTS-xBNN) lead-free piezoelectric ceramics have been prepared using a conventional solid-state reaction method and the effects of BNN on their phase structure, microstructure, and electrical properties systematically studied. X-ray diffraction analysis suggested that BNN substitution into KNLNTS induced coexistence of orthorhombic–tetragonal mixed phase and thus improved the ferroelectric and piezoelectric properties. The surface morphologies indicated that different amounts of BNN had two different effects on grain growth. Good electrical properties (d_{33} = 256 pC N^{-1}, T_c = 354.27°C, k_p = 43.43%, P_r = 26.85 μC cm^{-2}, E_c = 24.47 kV cm^{-1}) were simultaneously obtained at x = 0.0025, suggesting that our research could benefit development of (K,Na)NbO_3-based ceramics and widen their application range.

Key words: Lead-free, piezoelectric ceramics, microstructure, electrical properties

INTRODUCTION

Piezoelectric materials have been widely used in the field of energy conversion, e.g., in actuators, transducers, and sensors, and related studies lie at the forefront of high-technology advanced materials research.[1] Over the last five decades, lead zirconate titanate (PZT) has dominated most piezoelectric applications due to its high piezoelectric response, large-scale production capability, and the possibility of adjusting the composition to tailor its properties, which are closely related to the chemical structure of Pb.[2] Meanwhile, lead 6*s* and O 2*p* states are strongly hybridized, leading to large strain that stabilizes the tetragonal phase, playing an important role in the piezoresponse of PZT ceramics.[3] However, PZT has high lead content of ~60%, which may cause serious damage to the environment or humans during preparation, processing, and even disposal.[4–8] Therefore, it is necessary to develop lead-free piezoelectric ceramics with excellent properties as substitutes for lead-based ceramics in various devices.[9]

$(K_{0.5}Na_{0.5})NbO_3$ (KNN) ceramics have received much attention because of their high Curie temperature and good piezoelectric and mechanical properties.[10–16] They have now become some of the most promising candidates to replace PZT-based ceramics.[17–20] However, a few drawbacks still prevent wide-scale industrial use of KNN ceramics, owing to their poor sintered density due to the volatility of alkaline elements at high temperatures and the hygroscopic nature of the reactant powders. Much research work has been carried out to improve the sintering performance and electrical properties of KNN ceramics; For example, high piezoelectric constant d_{33} (~416 pC N^{-1}) was achieved in 2004 in KNN ceramics doped with Ta, Sb, and Li using a complicated reaction template grain growth (RTGG)

(Received May 25, 2016; accepted August 9, 2016; published online August 24, 2016)

method.[5] This achievement indicated that high d_{33} is attainable in the KNN system. Since then, some researchers have begun to explore various approaches to optimize the properties of KNN materials. These approaches include substitution modification such as adding a second component or sintering additives, and novel preparation technology.[4–6,21–25] Recently, the relationships between their phase boundary and electric properties have been investigated to realize further breakthroughs.[4,5,21–23] The research group at Sichuan University made a significant breakthrough in KNN-based ceramics using a conventional solid-state method, achieving giant piezoelectricity with extremely high piezoelectric constant $d_{33} > 360$ pC N^{-1},[26–29] indicating that there is plenty of room for improvement of KNN-based ceramics.

It is also known that shifting the orthorhombic–tetragonal phase-transition temperature (T_{o-t}) to near room temperature is a common way to improve the electrical properties of KNN ceramics.[30] In previous reports, $Bi_{0.5}K_{0.5}ZrO_3$ was selected to shift T_{o-t} to near room temperature.[31,32] $(Bi_{0.5}Na_{0.5})TiO_3$ (BNT) is also considered an excellent candidate lead-free piezoelectric ceramic because of its strong ferroelectricity at room temperature and high Curie temperature; due to the similar ionic radii of Ti^{4+} (0.74 Å, CN = 8) and Nb^{5+} (0.74 Å, CN = 8), Nb^{5+} can substitute at B-site of BNT. Many recent research studies have also focused on development of Bi-based piezoelectrics[9] as environmentally compatible alternatives to PZT, since Bi^{3+}, like the Pb^{2+} ion, is highly polarizable due to a lone electron pair.[33] For the reasons mentioned above, $Bi_{0.25}Na_{0.25}NbO_3$ (BNN) theoretically has the ability to improve the electrical properties of KNN ceramics. Study of KNN ceramics partially substituted with Li^+, Ta^{5+}, and Sb^{5+} has revealed that the composition $(Na_{0.52}K_{0.44}Li_{0.04})(Nb_{0.87}Sb_{0.08}Ta_{0.05})O_3$ (KNLNTS) possesses the highest values.[8] This was therefore chosen as our base composition for this work. To obtain KNN-doped ceramics with good electrical properties, ceramics with a series of compositions KNLNTS-xBNN were prepared by a conventional solid-state method, and the effects of the BNN content on their phase structure, microstructure, and electrical properties were investigated.

EXPERIMENTAL PROCEDURES

KNLNTS-xBNN (x = 0 to 0.008) piezoelectric ceramics were synthesized by a conventional solid-state reaction method using Na_2CO_3 (99.8%), K_2CO_3 (99%), Ta_2O_5 (99.99%), Li_2CO_3 (98%), Nb_2O_5 (99.5%), Sb_2O_3 (99%), and Bi_2O_3 (99.99%) as starting materials. These powder mixtures were ball-milled for 12 h in ethanol with zirconia balls as milling medium. The slurries were dried and calcined at 850°C for 2 h. After calcination, the mixtures were milled again for 12 h. The obtained powders were then mixed with an appropriate amount of polyvinyl butyral (PVB) binder, and pressed into pellets with diameter of 12 mm and thickness of 1.0 mm under pressure of about 200 MPa. After burning off PVB, the ceramics were sintered at 1130°C, 1120°C, 1115°C, and 1110°C for 2 h in air.

The crystal structure of the sintered ceramics was determined by x-ray powder diffraction (XRD) analysis (D8 Advance, Bruker Inc., Germany). The surface morphology of the ceramics was studied by scanning electron microscopy (SEM; JSM-6380, Japan). For electrical measurements, silver paste was coated on both sides of the sintered samples and fired at 740°C for 20 min to produce electrodes. The temperature-dependent dielectric properties were measured using a broadband dielectric spectrometer (Novocontrol, Germany). The electric-field-induced polarization (P–E) was measured using a TF2000FE-HV ferroelectric test unit (aix-ACCT Inc. Germany). Piezoelectric measurements were carried out using a quasistatic d_{33}-meter (YE2730; SINOCERA, China). Before measurements, the samples were poled in silicone oil at room temperature under 50 kV cm^{-1} to 70 kV cm^{-1} for 20 min. The planar electromechanical coupling factor k_p was calculated using the following equations based on measurements with an impedance analyzer (Agilent 4294A)[34]:

$$\frac{1}{k_p^2} = 0.395\frac{f_r}{f_a - f_r} + 0.574, \quad (1)$$

where f_r and f_a are the resonance and antiresonance frequency, respectively.

RESULTS AND DISCUSSION

Figure 1a shows the XRD patterns of the KNLNTS-xBNN ceramics in the 2θ range from 20° to 70°. All the ceramics possessed pure perovskite structure without any secondary phases, suggesting that BNN diffused into the KNLNTS lattice to form a homogeneous solid solution for the present doping concentrations. The ceramics with $x < 0.0025$ possessed tetragonal structure with splitting of the (001)/(100) and (002)/(200) characteristic peaks.[35] Ceramics with $0.0025 \le x \le 0.003$ exhibited coexistence of orthorhombic and tetragonal phase structures, because their T_{o-t} value is about 70°C;[36–39] furthermore, the samples with $x > 0.003$ exhibited dominant tetragonal structure.

To clearly analyze the effects of BNN on the phase structure of all samples, expanded XRD patterns of the KNLNTS-xBNN ceramics in the 2θ ranges of 30° to 34° and 47° to 56° are shown in Fig. 1b and c, respectively. It can be noted that the diffraction peaks shift slightly to lower angle for $x < 0.0025$, suggesting that the volume of the crystal cell enlarges with an increase of the BNN content. This

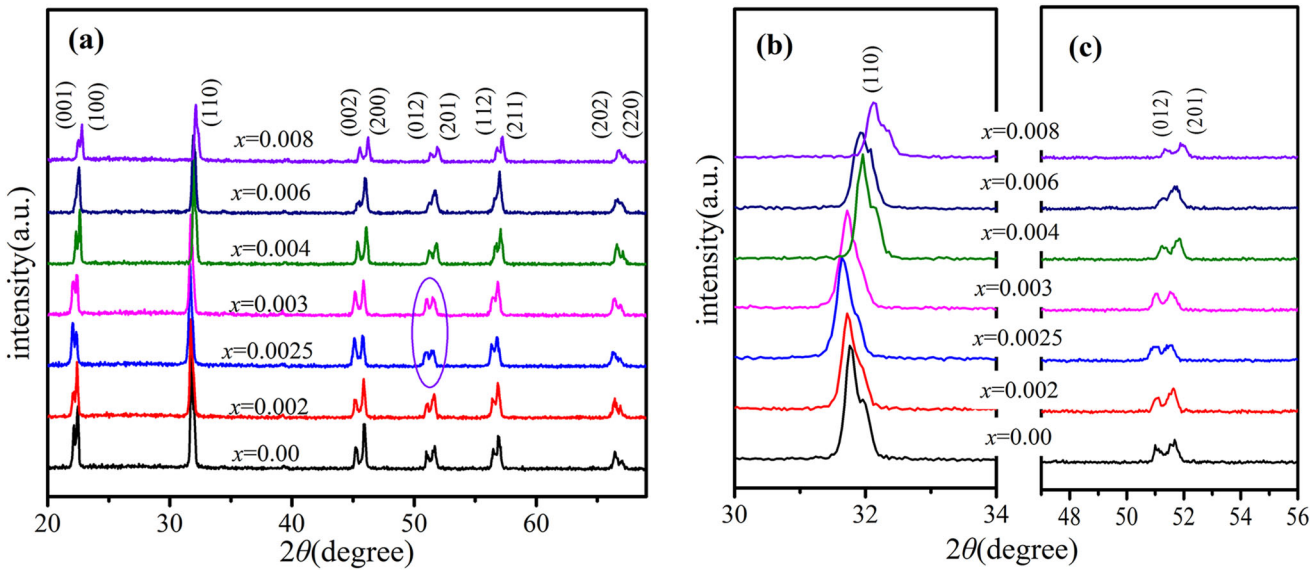

Fig. 1. XRD patterns of KNLNTS-xBNN ceramics in the 2θ range of (a) 20° to 70°, (b) 30° to 34°, and (c) 47° to 56°.

variation is attributed to substitution of Li^+ (0.76 Å, CN = 6) cations by Na^+ ions (1.02 Å, CN = 6).[39] Also, the diffraction peaks shift slightly to higher diffraction angle for $x \geq 0.0025$, illustrating decreased lattice spacing owing to the relatively smaller ionic radius of Bi^{3+} (1.03 Å, CN = 6) and its higher ion valence compared with K^+ (1.38 Å, CN = 6) or Na^+ ion (1.02 Å, CN = 6), resulting in lattice contraction.[40] These results indicate that Bi^{3+} entered A-site of KNLNTS to substitute K^+ or Na^+ based on radius matching, while the differences in ionic radius resulted in lattice deformation at the same time.

Figure 2 shows the surface morphology of the ceramics as a function of x. It is seen that all ceramics were well sintered and considerably dense. Moreover, it was also found that the grain size of the ceramics increased for $x < 0.004$, then gradually decreased for $x \geq 0.004$. This phenomenon indicates that different amounts of BNN had two different effects on grain growth. With less BNN, promotion of grain growth was the main effect. The grain distribution may be due to addition of Bi^{3+}, which can improve the migration rate of grain boundaries, thus accelerating the grain growth of the KNLNTS ceramics owing to the involved liquid phases.[30] However, the grain size reduced slightly with further increase of the BNN content. This can probably be explained by the following two reasons: (1) Large BNN addition could cause precipitation of excess Bi_2O_3 at grain boundaries, hindering their movement and inhibiting grain growth.[41] (2) Another reason may be the lower sintering temperature.[42] Stable solid solutions together with dense microstructure can then be formed, as smaller grains gather into the gaps among larger ones. Therefore, the amount of BNN doping had a significant influence on the grain growth.

Figure 3a shows the temperature dependence of the dielectric permittivity ε_r and dielectric loss tan δ for the KNLNTS-xBNN samples, obtained at measuring frequency of 1 kHz. It can be seen that all the samples exhibited two dielectric peaks, at about 70°C and 350°C, corresponding to the orthorhombic–tetragonal (at T_{o-t}) and tetragonal–cubic (at T_c) phase transition, respectively. The variations in T_{o-t} and T_c with x for the ceramics are shown in Fig. 3b. T_c was observed to increase from 351°C to 354°C as x was increased from 0.002 to 0.0025, then to decrease to 330°C for $x = 0.004$. T_{o-t} decreased from 109°C to 57°C as x was increased from 0.002 to 0.004. These slight changes in T_{o-t} and T_c should be attributed to valence mismatch.[43–45] In this work, addition of Bi^{3+} easily resulted in valence mismatch at A-site of KNLNTS ceramic. Therefore, the phase transition shifts to lower temperature with increasing BNN content.[39] Although the KNLNTS-xBNN ceramics exhibited T_{o-t} values above room temperature, the transition from the tetragonal to orthorhombic phase was gradual, hence the ceramics should contain a small fraction of tetragonal as well as orthorhombic phase at room temperature. The dielectric loss was relatively lower from room temperature up to 300°C, reaching a peak at around T_c, after which it increased rapidly as a result of conductive losses. The dielectric permittivity ε_r of the studied ceramics measured at 1 kHz, 10 kHz, and 100 kHz as functions of temperature in the range from 25°C to 550°C are shown in Fig. 4. Strong frequency dispersion of the dielectric permittivity is clearly found. The maximum dielectric permittivity ε_r decreased while the transition temperature increased slightly with increasing frequency. The nature of the diffuse phase transition and the frequency dispersion indicate that the diffuseness was enhanced by introducing Bi, and

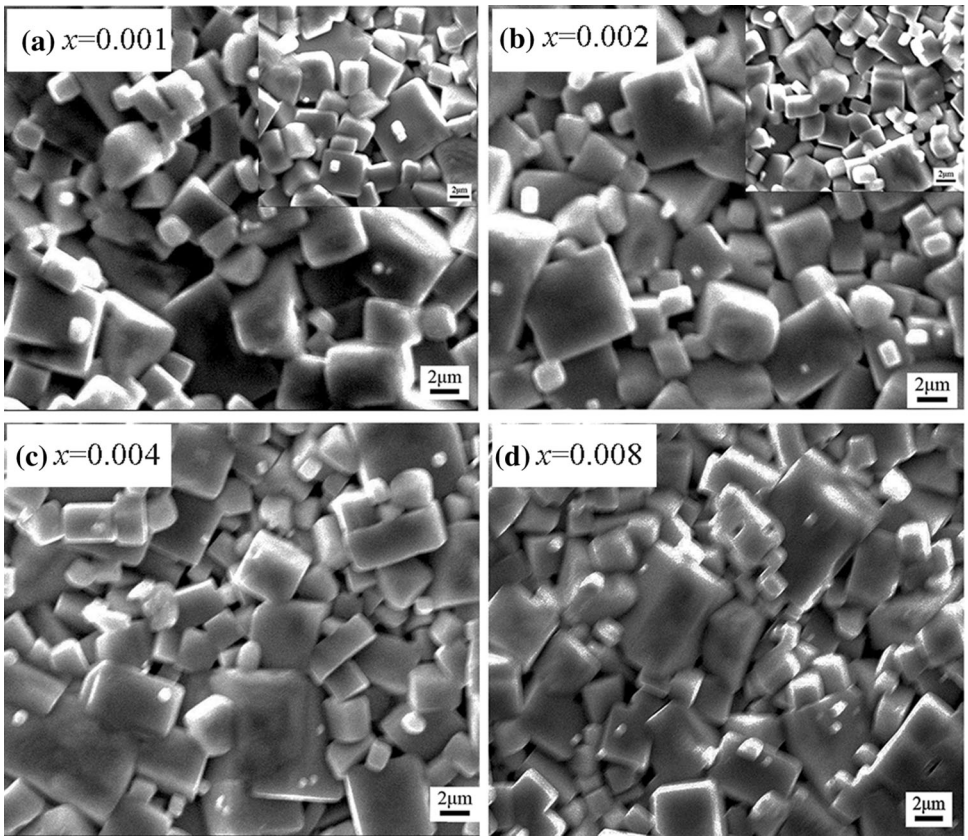

Fig. 2. SEM micrographs of KNLNTS-*x*BNN ceramics with different BNN contents sintered at 1130°C for 2 h.

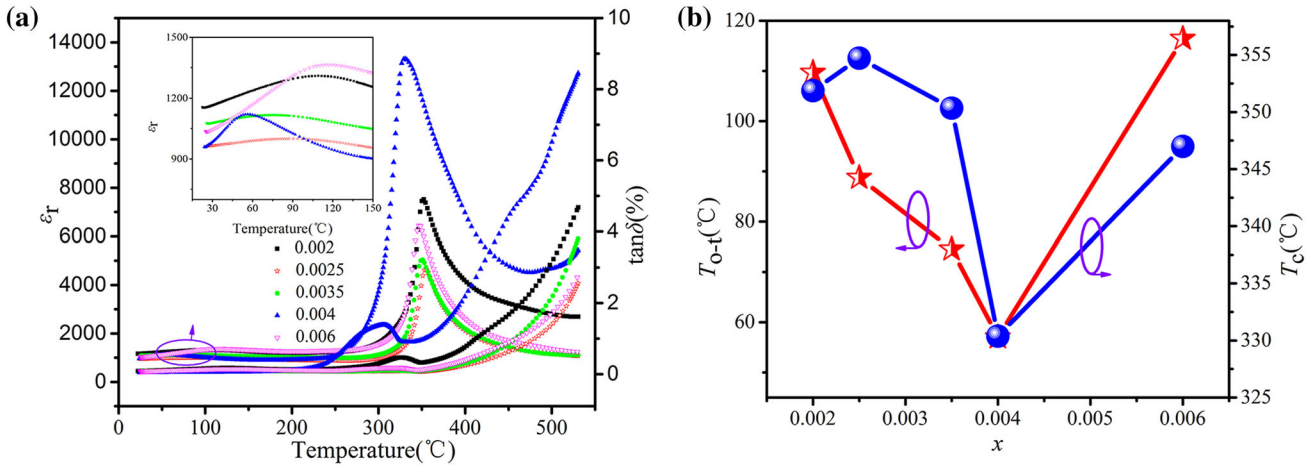

Fig. 3. (a) Dielectric permittivity ε_r and dielectric loss tan δ as functions of temperature for KNLNTS-*x* BNN ceramics at 1 kHz. (b) Variations of T_c and T_{o-t} with *x* for the KNLNTS-*x*BNN ceramics.

furthermore that the KNLNTS-*x*BNN ceramics underwent a change from a normal to a relaxor-like ferroelectric as the Bi content was increased.[37]

Hysteresis loops (*P*–*E*) of the KNLNTS-*x*BNN ceramics measured at 10 Hz and room temperature are depicted in Fig. 5a. All samples showed typical *P*–*E* hysteresis loops. To further understand their ferroelectric properties, we plot the composition dependence of the remanent polarization (P_r) and coercive field (E_c) in Fig. 5b. Both P_r and E_c were found to show the same trend with composition. P_r changed little for different *x* values. The composition with $x = 0.003$ showed the optimum ferroelectric properties, with low value of E_c, as follows: $P_r = 26.85\ \mu C\ cm^{-2}$ and $E_c = 24.47\ kV\ cm^{-1}$. In general, the piezoelectric properties of a

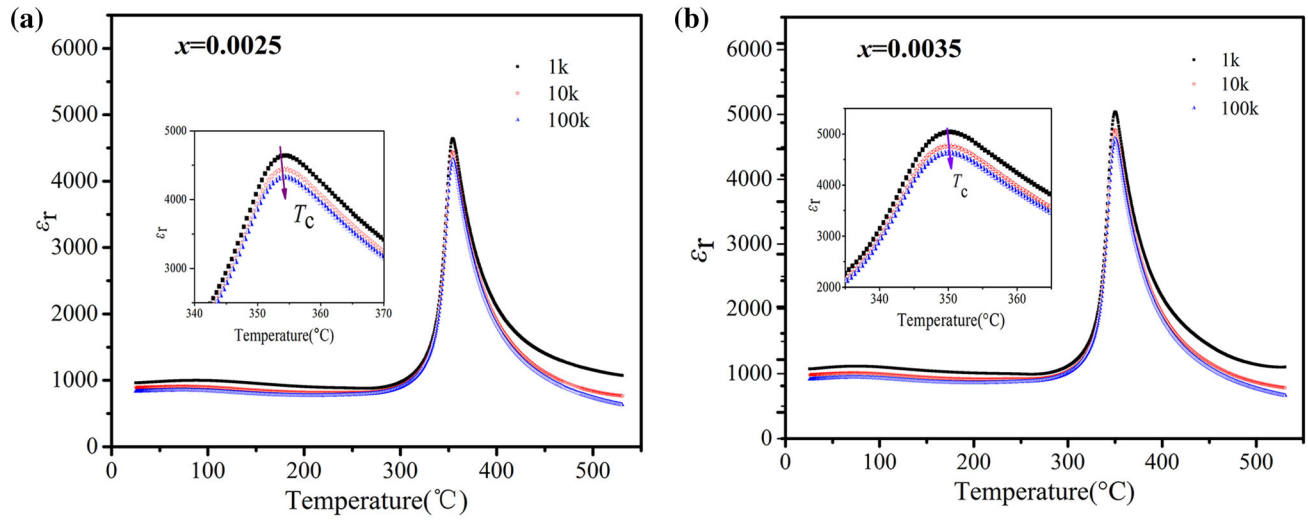

Fig. 4. Temperature dependence of dielectric permittivity and loss tangent for KNLNTS-*x*BNN samples with (a) $x = 0.0025$ and (b) $x = 0.0035$, at measuring frequency from 1 kHz to 100 kHz.

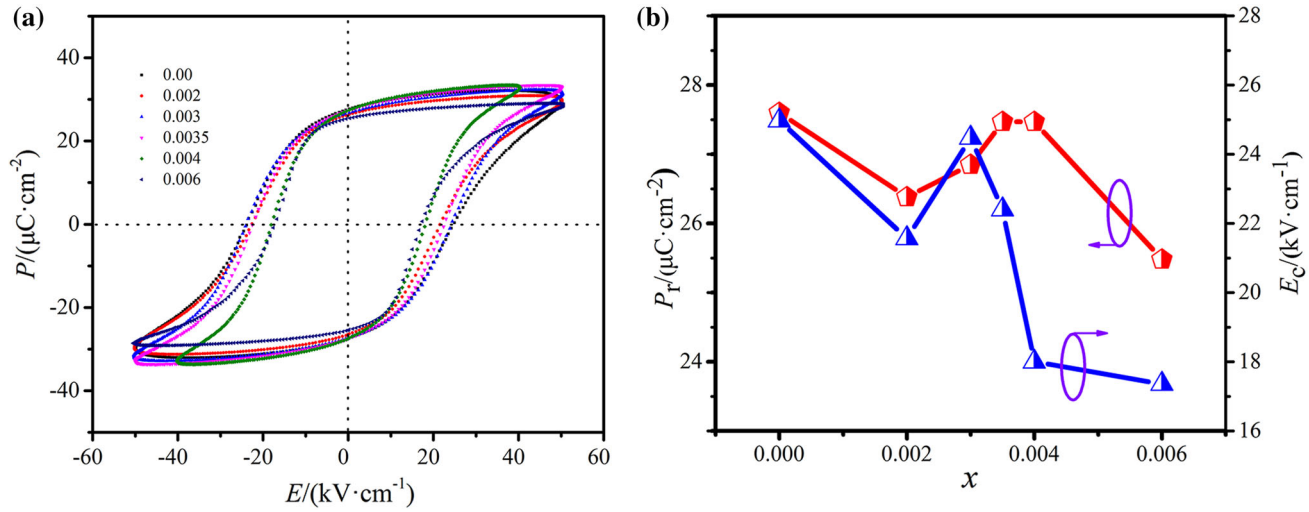

Fig. 5. (a) *P*–*E* hysteresis loops of KNLNTS-*x*BNN samples measured at 10 Hz and room temperature. (b) Variations of P_r and E_c of the KNLNTS-*x*BNN ceramics as functions of *x*.

ferroelectric material are related to two factors: P_r and E_c. Piezoelectric ceramics with higher P_r possess higher piezoelectric properties, because higher P_r indicates a higher degree of ferroelectric domain orientation. On the other hand, lower E_c can facilitate domain movement, resulting in improved piezoelectric properties. Consequently, piezoelectric ceramics with higher P_r and lower E_c generally possess higher piezoelectric properties.[46] The ceramic with $x = 0.003$ showed the optimum piezoelectric properties owing to the coexistence of the orthorhombic and tetragonal phases in this system, as discussed in Fig. 6.

Figure 6 shows the composition dependence of the piezoelectric coefficient (d_{33}) and electromechanical coupling factor (k_p) for the KNLNTS-*x*BNN ceramics. It is observed that both d_{33} and k_p show a similar tendency. The ceramics reach the highest d_{33} value of 256 pC N^{-1} and k_p of 43.43% at $x = 0.0025$. These values are much higher than those ($d_{33} \approx 80$ pC N^{-1} and $k_p \approx 23.2\%$) of pure KNN.[47] As mentioned above, the composition with $x = 0.0025$ lies near the tetragonal–orthorhombic region. Therefore, its enhanced electrical properties can be attributed to the phase transition from tetragonal to orthorhombic symmetry, where polarization rotation occurs among many more polarization states.[25] However, d_{33} and k_p dwindled rapidly with excess BNN content. This may because a large amount of BNN addition would lead to drastic worsening of the sintering behavior as well as pore formation in the ceramic bulk. Moreover, the

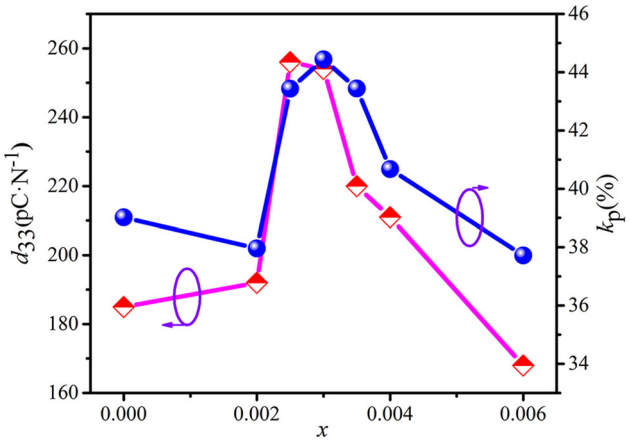

Fig. 6. Piezoelectric constant d_{33} and planar electromechanical coefficient k_p of the KNLNTS-x BNN ceramics as functions of x.

decrease of the grain size with excess BNN may lead to deterioration of the piezoelectric properties.[48,49] As a result, moderate addition of BNN could enhance the piezoelectric properties of the KNN material.

CONCLUSIONS

KNLNTS-xBNN lead-free piezoelectric ceramics were prepared using a conventional solid-state sintering method, and the effects of BNN on their phase structure, microstructure, and electrical properties systematically studied. All compositions had pure perovskite structure. Both orthorhombic and tetragonal ferroelectric phases coexisted in the crystal structure of the ceramics with $0.0025 \le x \le 0.003$. The BNN-modified ceramics showed clear grain boundaries and uniformly distributed grain size. The dielectric, ferroelectric, and piezoelectric properties were correspondingly improved in the range of mixed phases. The composition with $x = 0.0025$ showed the optimum electric properties: $d_{33} = 256$ pC N^{-1}, $T_c = 354.27$°C, $k_p = 43.43\%$, $P_r = 26.85$ μC cm^{-2}, $E_c = 24.47$ kV cm^{-1}, demonstrating the potential of this new method to obtain high-performance potassium–sodium niobate materials.

ACKNOWLEDGEMENTS

This work was supported by the National Natural Science Foundation of China (Nos. 51372110, 51402144, 51302124, 51302025), Science and Technology Planning Project of Guangdong Province, China (No. 2013B091000001), Independent innovation and achievement transformation in Shandong Province special, China (No. 2014CGZH0904), The Project of Shandong Province Higher Educational Science and Technology Program (Nos. J14LA11, J14LA10), and the Research Foundation of Liaocheng University (Nos. 318011301, 318011306).

REFERENCES

1. J.F. Li, K. Wang, F.Y. Zhu, L.Q. Cheng, and F.Z. Yao, *J. Am. Ceram. Soc.* 12, 3677 (2013).
2. A. Tian, Z. Xu, S. Liu, N. Jiang, and H. Du, *J. Chin. Ceram. Soc.* 42, 667 (2014).
3. R.E. Cohen, *Nature* 358, 136 (1992).
4. J. Wu, D. Xiao, and J. Zhu, *Chem. Rev.* 115, 2559 (2015).
5. Y. Saito, H. Takao, T. Tani, T. Nonoyama, K. Takatori, T. Homma, T. Nagaya, and M. Nakamura, *Nature* 432, 84 (2004).
6. J. Rödel, W. Jo, K.T. Seifert, E.M. Anton, T. Granzow, and D. Damjanovic, *J. Am. Ceram. Soc.* 92, 1153 (2009).
7. L. Bellaiche, A. García, and D. Vanderbilt, *Phys. Rev. Lett.* 84, 5427 (2000).
8. J. Du, G. Zang, X. Yi, Z. Xu, R. Chu, C. Ban, and Y. Wei, *Mater. Lett.* 79, 89 (2012).
9. T.R. Shrout and S.J. Zhang, *J. Electroceram.* 19, 113 (2007).
10. H. Wang, X. Zhai, J. Xu, C. Yuan, and L. Yang, *J. Electron. Mater.* 42, 2556 (2013).
11. J.-J. Zhou, J.-F. Li, K. Wang, and X.-W. Zhang, *J. Mater. Sci.* 46, 5111 (2011).
12. R. Bathelt, T. Soller, K. Benkert, C. Schuh, and A. Roosen, *J. Eur. Ceram. Soc.* 32, 3767 (2012).
13. W. Liang, W. Wu, D. Xiao, J. Zhu, and J. Wu, *J. Mater. Sci.* 46, 6871 (2011).
14. J. Fu, R. Zuo, and Y. Liu, *J. Alloys Compd.* 493, 197 (2010).
15. H. Zhang, S. Yang, S. Yang, D. Kong, B.-P. Zhang, and Y. Zhang, *J. Eur. Ceram. Soc.* 31, 795 (2011).
16. R. Cheng, C. Wang, Z. Xu, R. Chu, J. Hao, H. Li, W. Li, J. Du, and G. Li, *RSC Adv.* 5, 90508 (2015).
17. J.F. Li, K. Wang, B.P. Zhang, and L.M. Zhang, *J. Am. Ceram. Soc.* 89, 706 (2006).
18. S. Su, R. Zuo, X. Wang, and L. Li, *Mater. Res. Bull.* 45, 124 (2010).
19. H. Wang, D. Ruan, Y.-J. Dai, and X.-W. Zhang, *Curr. Appl. Phys.* 12, 504 (2012).
20. X. Wang, J. Wu, D. Xiao, X. Cheng, T. Zheng, X. Lou, B. Zhang, and J. Zhu, *ACS Appl. Mater. Interfaces* 6, 6177 (2014).
21. T. Zheng, J. Wu, X. Cheng, X. Wang, B. Zhang, D. Xiao, J. Zhu, and X. Lou, *Dalton Trans.* 43, 9419 (2014).
22. K. Wang and J.F. Li, *Adv. Funct. Mater.* 20, 1924 (2010).
23. R. Zuo, J. Fu, and D. Lv, *J. Am. Ceram. Soc.* 92, 283 (2009).
24. T. Zheng, J. Wu, D. Xiao, J. Zhu, X. Wang, L. Xin, and X. Lou, *ACS Appl. Mater. Interfaces* 7, 5927 (2015).
25. J. Wu, Y. Wang, and H. Wang, *RSC Adv.* 4, 64835 (2014).
26. X. Cheng, J. Wu, X. Wang, B. Zhang, J. Zhu, D. Xiao, X. Wang, and X. Lou, *Appl. Phys. Lett.* 103, 052906 (2013).
27. X. Wang, J. Wu, D. Xiao, J. Zhu, X. Cheng, T. Zheng, B. Zhang, X. Lou, and X. Wang, *J. Am. Ceram. Soc.* 136, 2905 (2014).
28. X. Cheng, J. Wu, X. Lou, X. Wang, X. Wang, D. Xiao, and J. Zhu, *ACS Appl. Mater. Interfaces* 6, 750 (2014).
29. J. Hao, Z. Xu, R. Chu, W. Li, and P. Fu, *Mater. Res. Bull.* 65, 94 (2015).
30. S.H. Park, C.W. Ahn, S. Nahm, and J.S. Song, *Jpn. J. Appl. Phys.* 43, 1072 (2004).
31. R. Zuo, X. Fang, and C. Ye, *Appl. Phys. Lett.* 90, 092904 (2007).
32. M. Xiao, D. Xiao, Z. Wang, T. Huang, J. Wu, F. Li, B. Wu, and J. Zhu, *J. Mater. Sci. Mater. Electron.* 25, 1938 (2014).
33. M.R. Suchomel, A.M. Fogg, M. Allix, H.J. Niu, J.B. Claridge, and M.J. Rosseinsky, *Chem. Mater.* 18, 4987 (2006).
34. J. Hao, Z. Xu, R. Chu, Y. Zhang, Q. Chen, W. Li, P. Fu, G. Zang, G. Li, and Q. Yin, *J. Electron. Mater.* 39, 347 (2010).
35. F. Tang, H. Du, D. Liu, F. Luo, and W. Zhou, *J. Inorg. Mater.* 2, 323 (2007).
36. Y. Guo, K. Kakimoto, and H. Osato, *Appl. Phys. Lett.* 85, 4121 (2004).
37. J. Hao, Z. Xu, R. Chu, W. Li, G. Li, and Q. Yin, *J. Alloys Compd.* 484, 233 (2009).

38. J. Wu, Y. Wang, D. Xiao, J. Zhu, P. Yu, L. Wu, and W. Wu, *Jpn. J. Appl. Phys.* 46, 7375 (2007).
39. M. Sutapun, W. Vittayakorn, R. Muanghlua, and N. Vittayakorn, *Mater. Des.* 86, 564 (2015).
40. H. Liu, F. Du, F. Tang, Luo, and W. Zhou, *J. Chin. Ceram. Soc.* 35, 1141 (2007).
41. J. Du, J. Liu, Z. Xu, R. Chu, X. Yi, J. Hao, and W. Li, *J. Mater. Sci. Mater. Electron.* 26, 9654 (2015).
42. C. Jiten, R. Gaur, R. Laishram, and K.C. Singh, *Ceram. Int.* 10, 1016 (2016).
43. T.Y. Tien, E.C. Subbarao, and J. Hirzo, *J. Am. Ceram. Soc.* 45, 572 (1962).
44. R.J. Bratton and T.Y. Tien, *J. Am. Ceram. Soc.* 50, 90 (1967).
45. M. Wu, L. Fang, L. Liu, X. Zhou, Y. Huang, and Y. Li, *Mater. Chem. Phys.* 132, 1015 (2012).
46. H. Du, F. Tang, D. Liu, D. Zhu, W. Zhou, and S. Qu, *Mater. Sci. Eng. B Adv.* 136, 165 (2007).
47. E.K. Akdogan, K. Kerman, M. Abazari, and A. Safari, *Appl. Phys. Lett.* 92, 11 (2008).
48. W. Li, P. Li, H. Zeng, J. Hao, and J. Zhai, *Ceram. Int.* 29, 8 (2012).
49. V.R. Mudinepalli, L. Feng, W.C. Lin, and B.S. Murty, *J. Adv. Ceram.* 4, 46 (2015).